MATH0024 PDEs Homework 2

Loïc Delbarre (S215072)

1. Fourier Transform Verification of the Fundamental Solution for the 3D Wave Equation

The goal is to prove that $\langle \Phi_t, \hat{\varphi} \rangle = \left\langle \hat{\Phi}_t, \varphi \right\rangle$ for all Schwartz functions φ on $\mathbb{R}^3$
By definition,

$$\begin{aligned}
\langle \Phi_t, \hat{\varphi} \rangle &= \left\langle \Phi_t, \int_{\mathbb{R}^3} \exp(-i\boldsymbol{x} \cdot \boldsymbol{\xi}) \varphi(\boldsymbol{\xi}) d\boldsymbol{\xi} \right\rangle \\
&= \frac{t}{4\pi} \int_{\|y\|=1} \int_{\mathbb{R}^3} \exp(-ict\boldsymbol{y} \cdot \boldsymbol{\xi}) \varphi(\boldsymbol{\xi}) d\boldsymbol{\xi} dS_y \\
&= \int_{\mathbb{R}^3} \frac{t}{4\pi} \int_{\|y\|=1} \exp(-ict\boldsymbol{y} \cdot \boldsymbol{\xi}) dS_y \varphi(\boldsymbol{\xi}) d\boldsymbol{\xi} \\
&= \int_{\mathbb{R}^3} \frac{t}{4\pi} \int_{\|y\|=1} \exp(-ict y_3 \|\boldsymbol{\xi}\|) dS_y \varphi(\boldsymbol{\xi}) d\boldsymbol{\xi} \qquad (1)
\end{aligned}$$

By replacing it with spherical coordinates the inner integral becomes

$$\begin{aligned}
\int_{\|y\|=1} \exp(-ict y_3 \|\boldsymbol{\xi}\|) dS_y &= \int_0^{2\pi} \int_0^{\pi} \exp(-ict \cos(\theta) \|\boldsymbol{\xi}\|) \sin(\theta) d\theta d\chi \\
&= 2\pi \int_0^{\pi} \exp(-ict \cos(\theta) \|\boldsymbol{\xi}\|) \sin(\theta) d\theta \qquad (2)
\end{aligned}$$

By performing a substitution $p = \cos(\theta)$,where $dp = -\sin(\theta) d\theta$, we obtain

$$\begin{aligned}
2\pi \int_{-1}^{1} \exp(-ictp\|\boldsymbol{\xi}\|) dp &= 2\pi \left[\frac{\exp(-ictp\|\boldsymbol{\xi}\|)}{-ictp\|\boldsymbol{\xi}\|} \right]_{-1}^{1} \\
&= \frac{2\pi}{-ict\|\boldsymbol{\xi}\|} \left(e^{-ict\|\boldsymbol{\xi}\|} - e^{ict\|\boldsymbol{\xi}\|} \right) \\
&= \frac{4\pi \sin(ct\|\boldsymbol{\xi}\|)}{ct\|\boldsymbol{\xi}\|} \qquad (3)
\end{aligned}$$

> Therefore
>
> $$\begin{aligned}
> \langle \Phi_t, \hat{\varphi} \rangle &= \int_{\mathbb{R}^3} \frac{t}{4\pi} \cdot \frac{4\pi \sin(ct\|\boldsymbol{\xi}\|)}{ct\|\boldsymbol{\xi}\|} \varphi(\boldsymbol{\xi}) d\boldsymbol{\xi} \\
> &= \int_{\mathbb{R}^3} \frac{\sin(ct\|\boldsymbol{\xi}\|)}{c\|\boldsymbol{\xi}\|} \varphi(\boldsymbol{\xi}) d\boldsymbol{\xi} \qquad = \left\langle \hat{\Phi}_t, \varphi \right\rangle \qquad (4)
> \end{aligned}$$

2. Absolute Stability Analysis of the Forward Euler Method

This question will consider the forward Euler method for the initial-value problem

$$\begin{cases} \frac{du}{dt}(t) = \lambda u(t) & \text{for } t > 0, \qquad \lambda \in \mathbb{C} \\ u(0) = 1 & \text{at } t = 0 \end{cases} \qquad (5)$$

The exact solution is given by

$$u(t) = e^{\lambda t} \tag{6}$$

The forward euler method is given by

$$u_{n+1} = (1 + \triangle t \cdot \lambda) u_n \tag{7}$$

A time marching method is absolutely stable for a specific timestep $\triangle t$ if its application to this particular IVP leads for this timestep to a numerical solution with the same asymptotic behaviour.

$$u_n \to 0 \text{ as } n \to +\infty \text{ when } \mathrm{Re}(\lambda) < 0 \tag{8}$$

For the forward Euler method with initial condition,

$$|u_n| = |1 + \triangle t \cdot \lambda|^n \to 0 \text{ as } n \to +\infty \tag{9}$$

This requires

$$|1 + \triangle t \cdot \lambda| < 1 \tag{10}$$

The region of absolute stability (ie where the condition is respected) is a disk in the complex plane centered in (-1,0) with a radius of 1.
For $\lambda = -5$, the absolute stability inequation gives us:

$$-1 \leq 1 - 5 \triangle t \leq 1 \tag{11}$$

Where

- The upperbound is trivial for a positive $\triangle t$
- the lower bound gives $\triangle t \leq 0.4$

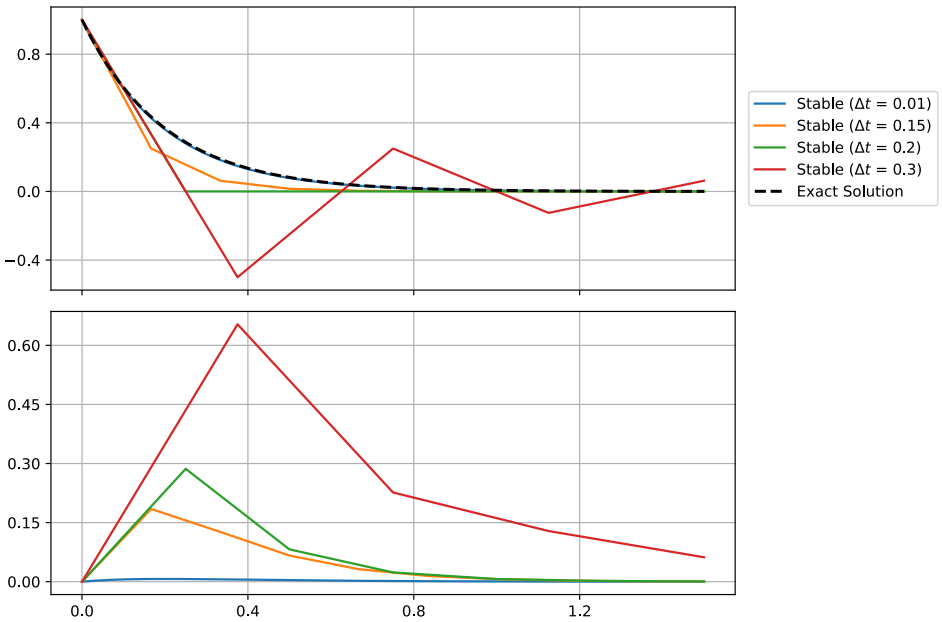

Figure 1: Representation of the forward Euler method and the representation of the absolute error associated to the method for $\triangle t$ in the stability interval.

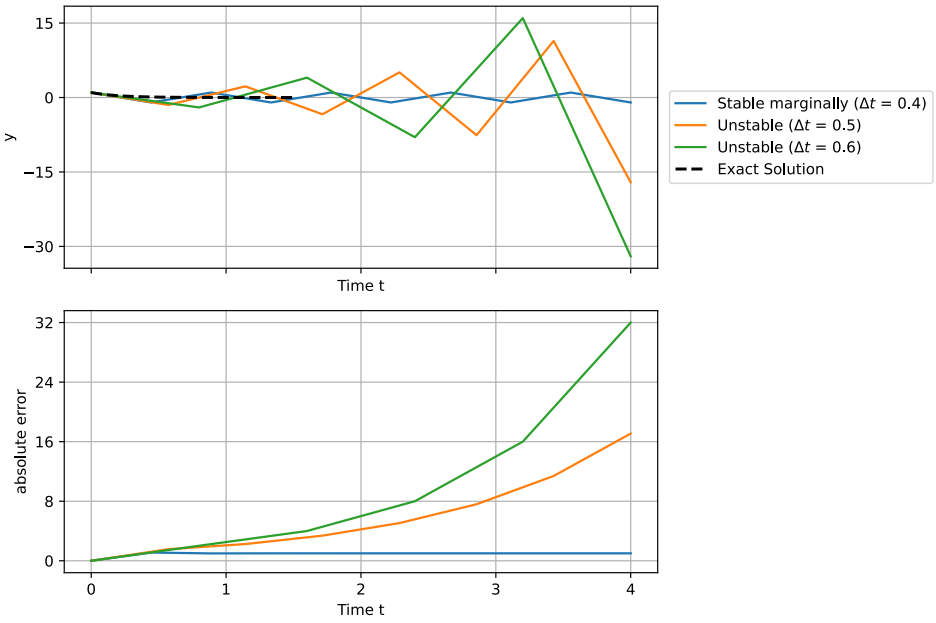

Figure 2: Representation of the forward Euler method and the representation of the absolute error associated to the method for unstable and stable marginally $\triangle t$

> The term $|1 + \triangle t \cdot \lambda|$ acts as the amplification factor. In the case of small value, the error will decay. In the case of $\triangle t = 0.4$, the scheme is marginally stable, the oscillation does not even grow or decay. After this limit value the amplification increases the amplitude of the oscillations. The absolute error explodes.

3. Spectral Analysis and Wave Propagation in Rectangular Waveguides

3.1. Spectral solution

The spectral problem equation is

$$-\frac{\partial^2 \phi}{\partial x^2} = \lambda \phi \tag{12}$$

Three cases must be discussed based on the sign of λ

- Case $\lambda < 0$

Let $\lambda = -\alpha^2$, with $\alpha > 0$
In this particular case the general solution is given by:

$$\varphi(x) = A\cosh(\alpha x) + B\sinh(\alpha x) \tag{13}$$

By applying the boundary condition

$$\begin{cases} \varphi\left(-\frac{L}{2}\right) = A\cosh\left(-\alpha\frac{L}{2}\right) + B\sinh\left(-\alpha\frac{L}{2}\right) = 0 \\ \varphi\left(\frac{L}{2}\right) = A\cosh\left(\alpha\frac{L}{2}\right) + B\sinh\left(\alpha\frac{L}{2}\right) = 0 \end{cases} \tag{14}$$

Knowing that sinh is a odd function and that cosh is even:

$$\begin{cases} \varphi(-\frac{L}{2}) = A\cosh(\alpha\frac{L}{2}) - B\sinh(\alpha\frac{L}{2}) = 0 \\ \varphi(\frac{L}{2}) = A\cosh(\alpha\frac{L}{2}) + B\sinh(\alpha\frac{L}{2}) = 0 \end{cases} \tag{15}$$

By rearranging, this gives

$$\begin{cases} 2A\cosh(\alpha\frac{L}{2}) = 0 \\ 2B\sinh(\alpha\frac{L}{2}) = 0 \end{cases} \tag{16}$$

That concludes that $A = B = 0$ and in extenso $\varphi(x) = 0$

- Case $\lambda = 0$

In this case the general solution is

$$\varphi(x) = Ax + b \tag{17}$$

By applying bondary condition;

$$\begin{cases} \varphi(-\frac{L}{2}) = -A\frac{L}{2} + B = 0 \\ \varphi(\frac{L}{2}) = A\frac{L}{2} + B = 0 \end{cases} \tag{18}$$

This situation also concludes that $A = B = 0$ and then that $\varphi(x) = 0$

- Case $\lambda > 0$

In this last case, the general solution is

$$\phi(x) = A\sin\left(\sqrt{\lambda}x\right) + B\cos\left(\sqrt{\lambda}x\right) \tag{19}$$

Using the bondary condition,

$$\begin{cases} \phi(-\frac{L}{2}) = 0 \\ \phi(\frac{L}{2}) = 0 \end{cases} \tag{20}$$

There is two sub-cases emerging

- $B = 0$ and $\sin\left(\sqrt{\lambda}\frac{L}{2}\right) = 0$

This conditions requires that

$$A\sin\left(\sqrt{\lambda}\frac{L}{2}\right) = 0$$

$$\lambda_m = \left(\frac{2m\pi}{L}\right)^2 \tag{21}$$

With $m \in \mathbb{N}_0^+$ The value m=0 is excluded as it gives the trivial solution, and negative values give the same eigenvalues as positive ones.

- $A = 0$ and $\cos\left(\frac{\sqrt{\lambda}L}{2}\right) = 0$

In this case

$$\lambda_k = \left(\frac{(2k+1)\pi}{L}\right)^2 \tag{22}$$

with $k \in \mathbb{N}_0^+$ To satisfy both boundary conditions with the domain centered at the origin, we use a phase-shifted representation.The complete set of eigenfunctions are :

$$\phi_m(x) = \sin\left(\frac{m\pi}{L}\left(x + \frac{L}{2}\right)\right) \tag{23}$$

By normalizing

$$\int_{-\frac{L}{2}}^{\frac{L}{2}} \sin^2\left(\frac{m\pi}{L}\left(x + \frac{L}{2}\right)\right)dx = \frac{L}{2} \tag{24}$$

> The solution to satisfy the bondary condition is then given by
>
> $$\phi_m(x) = \sqrt{\frac{2}{L}}\sin\left(\frac{m\pi}{L}\left(x + \frac{L}{2}\right)\right) \tag{25}$$
>
> For $m \in \mathbb{N}_0^+$

With the same analysis the y-direction problem gives with

$$\kappa_n = \left(\frac{n\pi}{H}\right)^2 \tag{26}$$

> The normalized form is given by
>
> $$\psi_n(y) = \sqrt{\frac{2}{H}}\sin\left(\frac{n\pi}{H}\left(y + \frac{H}{2}\right)\right) \tag{27}$$

3.2. Derivation in the sense of the theory of distribution

For all test function $\varphi \in \mathbb{R}$

$$\begin{aligned}\left\langle \frac{d}{dz}G_{mn}, \varphi \right\rangle &= -\left\langle G_{mn}, \frac{d}{dz}\varphi \right\rangle \\ &= -\int_{-\infty}^{+\infty} G_{mn}(z)\frac{d}{dz}\varphi dz = -\int_{-\infty}^{0} B_{mn}e^{-ik_{f,mn}z}\frac{d}{dz}\varphi dz \\ &\quad -\int_{0}^{+\infty} B_{mn}e^{ik_{f,mn}z}\frac{d}{dz}\varphi dz\end{aligned} \tag{28}$$

The integration by part returns

$$\begin{aligned}&= -\left[B_{mn}e^{-ik_{f,mn}z}\varphi\right]_{-\infty}^{0} + \int_{-\infty}^{0} B_{mn}\left(-ik_{f,mn}\right)e^{-ik_{f,mn}z}\varphi dz \\ &\quad -\left[B_{mn}e^{ik_{f,mn}z}\varphi\right]_{0}^{+\infty} + \int_{0}^{+\infty} B_{mn}\left(ik_{f,mn}\right)e^{ik_{f,mn}z}\varphi dz\end{aligned} \tag{29}$$

Since φ is a Schwartz function with compact support,it vanishes for $|x|$ sufficiently large,

$$\begin{aligned}&= -B_{mn}\varphi(0) + B_{mn}\varphi(0) + \int_{-\infty}^{0} B_{mn}\left(-ik_{f,mn}\right)e^{-ik_{f,mn}z}\varphi dz \\ &\quad + \int_{0}^{+\infty} B_{mn}\left(ik_{f,mn}\right)e^{ik_{f,mn}z}\varphi dz\end{aligned} \tag{30}$$

The first order derivative is then

$$\left\langle \frac{d}{dz}G_{mn},\varphi \right\rangle = \int_{-\infty}^{0} B_{mn}\big(-ik_{f,mn}\big)e^{-ik_{f,mn}z}\varphi dz + \int_{0}^{+\infty} B_{mn}\big(ik_{f,mn}\big)e^{ik_{f,mn}z}\varphi dz \quad (31)$$

The second order derivative can be obtain in the same way

$$\begin{aligned}\left\langle \frac{d^2}{dz^2}G_{mn},\varphi \right\rangle &= \left\langle G_{mn},\frac{d^2}{dz^2}\varphi \right\rangle \\ &= \int_{-\infty}^{+\infty} G_{mn}(z)\frac{d^2}{dz^2}\varphi dz \\ &= \int_{-\infty}^{0} B_{mn}e^{-ik_{f,mn}z}\frac{d^2}{dz^2}\varphi dz + \int_{0}^{+\infty} B_{mn}e^{ik_{f,mn}z}\frac{d^2}{dz^2}\varphi dz \end{aligned} \quad (32)$$

By decomposing the left integral (negative domain)

$$\begin{aligned}\int_{-\infty}^{0} B_{mn}e^{-ik_{f,mn}z}\frac{d^2}{dz^2}\varphi dz &= \left[B_{mn}e^{-ik_{f,mn}z}\frac{d}{dz}\varphi\right]_{-\infty}^{0} \\ &\quad - \int_{-\infty}^{0}\big(-ik_{f,nm}B_{mn}e^{-ik_{f,mn}z}\big)\frac{d}{dz}\varphi dz \\ = B_{mn}\frac{d}{dz}\varphi(0) + ik_{f,mn}B_{mn}\varphi(0) &+ \int_{-\infty}^{0}\big(-k_{f,mn}^2\big)B_{mn}e^{-ik_{f,nm}z}\varphi dz \end{aligned} \quad (33)$$

By doing the same thing developpement for the right integral (positive domain)

$$\begin{aligned}\int_{0}^{+\infty} B_{mn}e^{ik_{f,mn}z}\frac{d^2}{dz^2}\varphi dz &= -B_{mn}\frac{d}{dz}\varphi(0) + ik_{f,mn}B_{mn}\varphi(0) \\ &\quad + \int_{0}^{+\infty}\big(-k_{f,mn}^2\big)B_{mn}e^{ik_{f,mn}z}\varphi dz \end{aligned} \quad (34)$$

By adding both contribution

The second order derivative is then

$$\left\langle \frac{d^2}{dz^2}G_{mn},\varphi \right\rangle = -k_{f,mn}^2\langle G_{mn},\varphi\rangle + 2ik_{f,mn}B_{mn}\varphi(0) \quad (35)$$

3.3. Evaluation of B_{mn}

By substituing in the equation

$$-c^2\left[-k_{f,nm}^2G_{mn} + 2ik_{f,nm}B_{mn}\delta(z)\right] + \big(-\omega_f^2 + c^2(\lambda_m+\kappa_n)\big)G_{mn} = \phi_m(0)\psi_n(0)\delta(z) \quad (36)$$

Knowing that $k_{f,mn}^2 = \frac{\omega_f^2}{c^2} - (\lambda_m+\kappa_n)$

$$-2ic^2k_{\{f,mn\}}B_{\{mn\}}\delta(z) = \phi_m(0)\psi_n(0)\delta(z) \quad (37)$$

The value found is:

$$B_{mn} = i\frac{\phi_m(0)\psi_n(0)}{2c^2 k_{f,mn}} \tag{38}$$

4. Von Neuman Stability Analysis of the Upwind Finite Difference Scheme

4.1. Numerical Implementation and Error Observation

The upwind method is defined as

$$\begin{cases} u_j^{n+1} = u_j^n - c\frac{\triangle t}{h}\left(u_j^n - u_{j-1}^n\right) \\ u_j^0 = u_0(x_j) \end{cases} \tag{39}$$

Where $\nu = \frac{c\triangle t}{h}$
By assuming a solution on the form:

$$u_j = \gamma^n e^{i\xi jh} \tag{40}$$

The schema can be rewritten as

$$\begin{aligned} \gamma^{n+1}e^{i\xi jh} &= \gamma^n e^{i\xi jh} - \nu\gamma^n\left(e^{i\xi jh} - e^{i\xi(j-1)h}\right) \\ \gamma &= 1 - \nu\left(1 - e^{-i\xi h}\right) \end{aligned} \tag{41}$$

Since the transport equation propagates the initial profile unchanged at the velocity of $c = 1$, the exact solution at time t is given by

$$u(x,t) = \sin(2\pi(x-t)). \tag{42}$$

This represents a rightward-propagating wave that retains its shape and amplitude, exhibiting no dispersion. The comparison between the exact and numerical solutions in Figure 3 reveals characteristic numerical artifacts.
In Case 1, the numerical solution exhibits moderate amplitude reduction and slight phase lag relative to the exact solution, indicating the presence of both dissipation and dispersion errors. The dissipation error manifests as artificial damping of the wave amplitude, while the dispersion error causes different Fourier components to propagate at slightly different velocities, resulting in the observed phase shift.
Case 2, demonstrates significantly more pronounced numerical errors: the wave amplitude is severely attenuated and the phase lag is substantially larger, reflecting the coarser spatial resolution and larger time step. These observations align with the theoretical understanding that numerical errors accumulate more rapidly when the grid spacing increases, as the discrete approximation of spatial derivatives becomes less accurate.

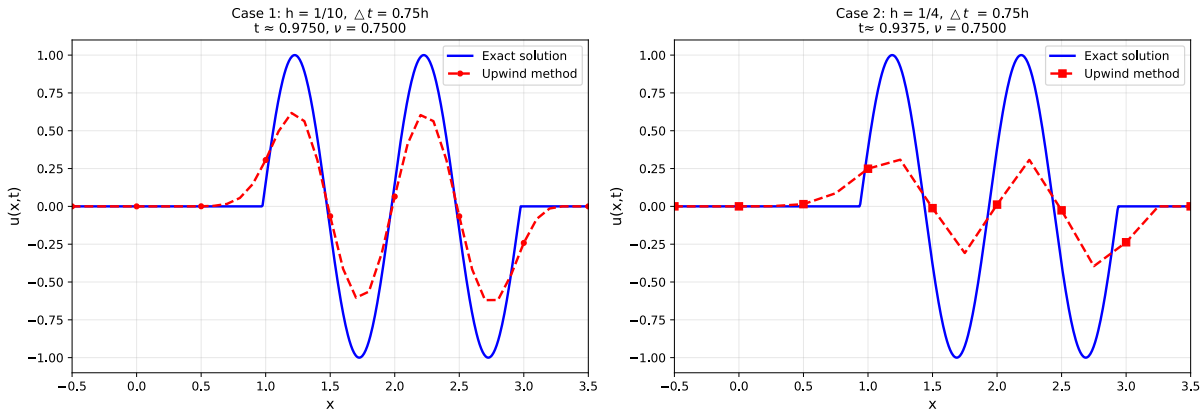

Figure 3: Comparison of exact and numerical solution for the transport equation at t≃1using the upwind finite difference method.

4.2. Spectral Analysis of Dissipation and Dispersion Errors

The Von Neumann analysis results from provide quantitative explanation for these observations. The amplification error plot (e_a) shows that $|\gamma(\xi)| < 1$ for all non-zero wavenumbers, confirming artificial dissipation across all Fourier modes, with higher wavenumbers experiencing greater damping.This directly accounts for the amplitude reduction observed in Section 4.1. The dispersion error plot (e_d) reveals that $e_d(\xi) < 1$ for $\xi \neq 0$, indicating that numerical wave components propagate slower than the exact solution, which explains the phase lag. Crucially, both error measures deteriorate more severely in Case 2 due to the coarser discretization (larger h means ξh spans a wider range of the error spectrum), confirming that the increased spatial step size amplifies both dissipation and dispersion effects.

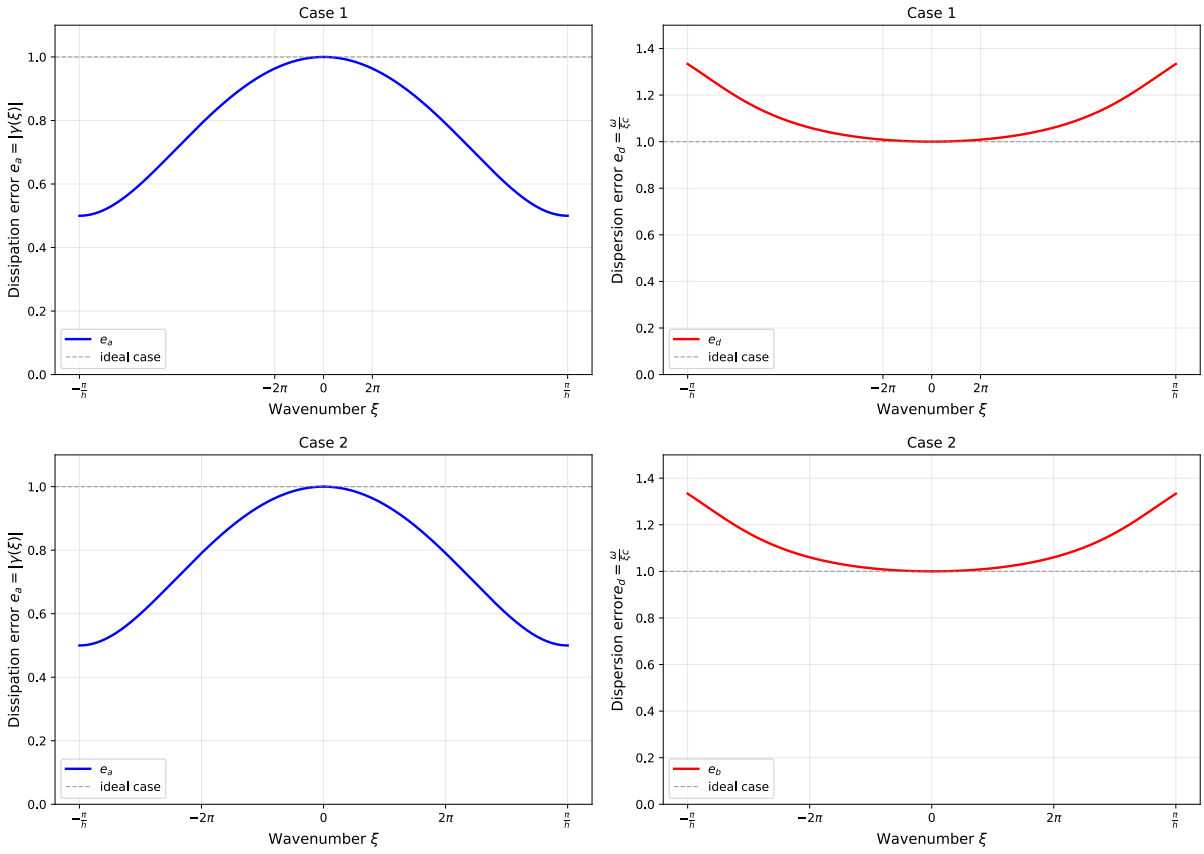

Figure 4: Von Neumann analysis of the upwind method, with dissipation e_a and dispersion e_d errors.

5. Use of AI

AI was used to summarise the instructions for question 3.